www.sciencemag.org/cgi/content/full/314/5802/1133/DC1

Supporting Online Material for

Solar Wind Neon from Genesis: Implications for the Lunar Noble Gas Record

Ansgar Grimberg,* Heinrich Baur, Peter Bochsler, Fritz Bühler, Donald S. Burnett, Charles C. Hays, Veronika S. Heber, Amy J. G. Jurewicz, Rainer Wieler

*To whom correspondience should be addressed. E-mail: grimberg@erdw.ethz.ch

Published 17 November 2006, *Science* **314**, 1133 (2006)
DOI: 10.1126/science.1133568

This PDF file includes:

Supporting Online Material

Materials and Methods:

Material: The collector material called Bulk Metallic Glass (BMG, Genesis target #40598) is an amorphous metal with a composition of $Zr_{58.5}Nb_{2.8}Cu_{15.6}Ni_{12.8}Al_{10.3}$ (atomic %). The nucleation of crystalline metal has been largely suppressed by rapidly quenching the liquid. Because there is no crystal lattice, fractionation and loss of trapped solar ions due to diffusion along preferred paths on crystal planes is reduced. Similarly, there are virtually no grain boundaries to provide fast-diffusion pathways. Therefore, the glass retains noble gases as neon well. Moreover, it etches very uniformly in HNO_3 and is therefore well suited for a stepwise gas release (*S1*).

Stepwise gas release: Neon was released by stepwise etching of the BMG surface with HNO_3 vapor. The closed system stepwise etching (CSSE) device in Zurich is directly connected to a noble gas mass spectrometer (*S1*). Sample and acid were stored in separate volumes under ultra high vacuum. Total amounts of ^{20}Ne released with CSSE and an achieved depth resolution of ~5-10 nm/step from sample 40958-03-F and 40958-03-B/04-K (Table S1) are in perfect agreement with amounts from total extraction given in Table S2.

Total extraction: Concentration and isotopic composition of the total Ne trapped in the BMG was determined by melting three samples of 7.7-8.7 mm^2 each at ~1500 °C, well above the BMG melting point. The released gas was analyzed in the same mass spectrometer as mentioned above. The values for all three samples are given in Table S2.

Modeling: Implantation of solar wind ions into the BMG was simulated using the SRIM code (*S2*). For each isotope the implantation depths and the fraction of backscattered particles lost from the target have been determined for 1.8×10^6 particles, assuming implantation of SW ions with a uniform $^{20}Ne/^{22}Ne$ ratio of 13.75 (see Table S2) over the entire SW energy range, which is supported by (*S3*), and a velocity distribution as measured with instruments onboard the advanced composition explorer (ACE) during the exposure time of Genesis (*S4*). The calculated backscattering correction for Ne into BMG is relatively high compared to a target like the Al-foils used in the Apollo experiment (*S5*), because the BMG consists to ~90% of heavy transition-metals. The adopted correction factors for the BMG are 1.014 for the $^{20}Ne/^{22}Ne$ ratio, 1.007 for the $^{21}Ne/^{22}Ne$ ratio and 1.13 for the ^{20}Ne amount.
To adapt this model to lunar grains two additional processes had to be introduced to account for the exposure conditions on the lunar surface. The first is sputtering of grain surfaces due to SW irradiation together with ongoing SW implantation on the freshly exposed surface. This was simulated until sputter-saturation equilibrium of the Ne isotopic composition was reached (after ~150 nm of surface sputtering). The second process considered was the production of Ne by spallation due to galactic cosmic rays (GCR). The isotopic composition of GCR-Ne was calculated using the model of (*S6*) for plagioclase chemistry and an assumed average shielding of <5 cm. The concentration of GCR-Ne added was chosen to yield a GCR-Ne/SW-Ne abundance ratio in the BMG similar to that found in lunar grains. In combination both processes shift SRIM results to SW-like values for surface-sited neon and to higher $^{21}Ne/^{22}Ne$ ratios in greater depth where SW ions are less abundant, leading to a slightly curved fractionation line that is hardly discernible from the straight line fit through the measured lunar data points for later steps.
Note that the $^{21}Ne/^{22}Ne$ ratio of the GCR point in Fig. 3 is slightly higher than in Fig. 1. Possibly this is partly due to the fact that the model by (*S6*) does not perfectly reproduce the isotopic composition of GCR-Ne or that the assumed mean shielding of <5 cm is not correct. However, it seems more likely that the linear extrapolation of the data points as indicated in Fig. 1 yields a slightly too low $^{21}Ne/^{22}Ne$ -GCR ratio, since the underlying assumption of a two-component mixing has proven in this paper to be wrong.

Supporting Figures:

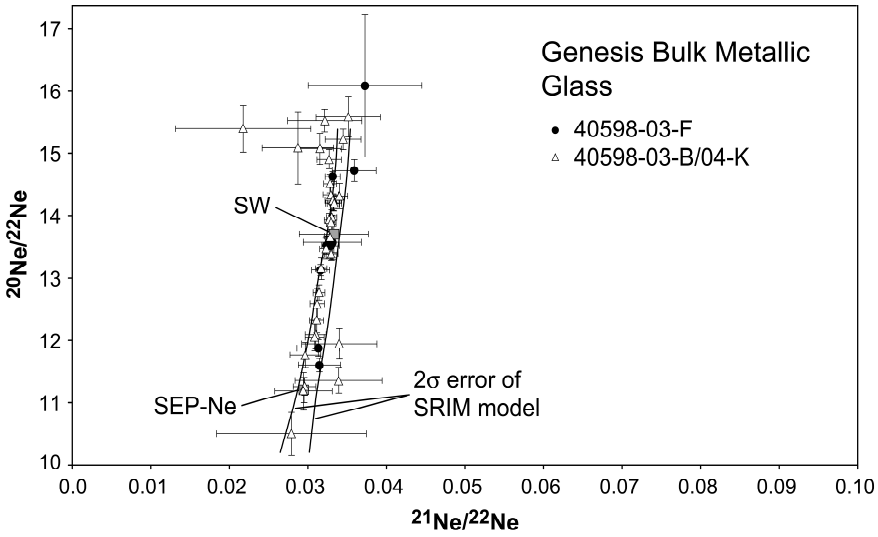

Figure S1: Ne three-isotope diagram from stepwise in-vacuo etching of Genesis bulk metallic glass sample (BMG). Data are for two etching-runs on the BMG (40958-03-F and 40958-03-B/04-K) exposed to the solar wind throughout the entire ~2.5 year Genesis exposure (Table S1). Data from the first steps (representing most superficially implanted gas) plot at $^{20}Ne/^{22}Ne$ ratios somewhat higher than the plotted SW value measured in Al foils during the Apollo lunar missions (*S5*). Large 2σ-error bars for some steps indicate very small amounts of gas released. Data from more deeply implanted Ne released in subsequent steps are aligned along a mass-dependent fractionation line. This trend is quantitatively described by fractionation during ion implantation, as shown by SRIM (*S2*) simulations plotted as its 2σ-envelope assuming implantation of a SW component with a velocity-independent $^{20}Ne/^{22}Ne$ ratio of 13.75±0.05 and $^{21}Ne/^{22}Ne$ ratio of 0.0330±0.0004 (average Table S2). The lowest measured $^{20}Ne/^{22}Ne$ ratios are similar to the SEP-Ne value reported from lunar samples (*S7*) plotted for reference. Overall the release pattern is similar to that from the lunar ilmenite (Fig. 1), apart from the fact that many lunar samples also release minor amounts of GCR-Ne, shifting especially the data points from later steps towards higher $^{21}Ne/^{22}Ne$ ratios.

Supporting Tables:

Sample 40598-03-F

Etching step	$^{20}Ne/^{22}Ne$	± 2σ	$^{21}Ne/^{22}Ne$ ($\times10^{-2}$)	± 2σ ($\times10^{-2}$)	^{20}Ne ($\times10^{9}$ atoms/cm^2)	± 2σ ($\times10^{9}$ atoms/cm^2)
1	16.08	1.14	3.73	0.72	5.31	0.22
2	14.72	0.18	3.59	0.28	90.46	3.51
3	14.62	0.08	3.32	0.10	150.38	5.84
4	14.19	0.12	3.32	0.08	286.31	10.83
5	13.56	0.29	3.31	0.37	19.62	0.75
6	13.52	0.15	3.24	0.06	281.97	1037
7	13.51	0.22	3.29	0.11	51.71	1.97
8	13.11	0.09	3.16	0.11	158.31	6.02
9	11.87	0.13	3.13	0.27	44.74	1.71
10	11.59	0.11	3.15	0.27	46.61	1.78
Total	13.67	0.09	3.27	0.05	1160	21
incl. backscattering	13.86	0.10	3.29	0.05	1311	23

Sample 40598-03-B/04-K

Etching step	$^{20}Ne/^{22}Ne$	± 2σ	$^{21}Ne/^{22}Ne$ ($\times10^{-2}$)	± 2σ ($\times10^{-2}$)	^{20}Ne ($\times10^{9}$ atoms/cm^2)	± 2σ ($\times10^{9}$ atoms/cm^2)
1	15.58	0.32	3.51	0.40	10.11	0.37
2	15.52	0.18	3.21	0.47	4.57	0.17
3	15.39	0.38	2.19	0.85	6.25	0.23
4	15.08	0.57	2.88	0.45	6.27	0.23
5	15.22	0.16	3.44	0.22	13.04	0.48
6	15.07	0.24	3.15	0.27	14.43	0.53
7	14.91	0.15	3.27	0.15	17.23	0.63
8	14.52	0.15	3.28	0.08	23.74	0.87
9	14.32	0.20	3.40	0.10	36.99	1.36
10	14.25	0.10	3.32	0.10	45.11	1.65
11	14.20	0.13	3.32	0.10	59.61	2.20
12	14.34	0.12	3.29	0.10	74.57	2.73
13	13.97	0.12	3.30	0.07	91.22	3.33
14	13.93	0.11	3.27	0.06	96.45	3.54
15	13.88	0.13	3.29	0.06	95.18	3.48
16	13.67	0.11	3.28	0.07	82.87	3.04
17	13.47	0.17	3.23	0.08	79.85	2.93
18	13.38	0.11	3.29	0.09	93.11	3.41
19	13.15	0.17	3.17	0.07	60.63	2.22
20	12.77	0.13	3.14	0.07	61.35	2.25
21	12.59	0.25	3.12	0.09	41.57	1.52
22	12.33	0.20	3.11	0.09	39.21	1.44
23	12.10	0.23	3.10	0.13	17.76	0.65
24	12.05	0.22	3.09	0.12	24.76	0.91
25	11.77	0.20	2.97	0.19	21.12	0.78
26	11.26	0.14	2.96	0.14	21.30	0.78
27	11.19	0.30	2.95	0.36	9.17	0.34
28	11.36	0.21	3.39	0.55	4.75	0.17
29	11.94	0.24	3.40	0.47	2.72	0.10
30	10.51	0.35	2.80	0.94	4.63	0.17
Total	13.65	0.06	3.28	0.05	1160	30
incl. backscattering	13.84	0.07	3.31	0.05	1311	33

Table S1: Ne concentrations and isotopic ratios measured by stepwise etching of samples 40598-03-F and 40598-03-B/04-K. The data shown for each single step and the respective total value are not corrected for losses due to backscattering. 2σ-errors include ion statistics, variations in sensitivity, interference corrections and uncertainties in the absolute calibration. Factors for the backscattering corrected total values are similar as described above. The average of values corrected for backscattering of both etching-runs is 13.85±0.11 for the $^{20}Ne/^{22}Ne$ ratio, 0.0330±0.0004 for the $^{21}Ne/^{22}Ne$ ratio and $(1.31\pm0.03)\times10^{12}$ for the ^{20}Ne amount.

Sample	$^{20}Ne/^{22}Ne$	± 2σ	$^{21}Ne/^{22}Ne$ ($\times 10^{-2}$)	± 2σ ($\times 10^{-2}$)	^{20}Ne ($\times 10^{9}$ atoms/cm^2)	± 2σ ($\times 10^{9}$ atoms/cm^2)
40598-03-C	13.52	0.08	3.25	0.05	1204	26
40598-03-D	13.61	0.07	3.28	0.12	1072	23
40598-03-E	13.54	0.07	3.31	0.09	1132	24
Average	13.56	0.05	3.28	0.04	1136	76
incl. backscattering	13.75	0.05	3.30	0.04	1284	90

Table S2: Ne concentrations and isotopic ratios measured by total extraction of samples 40598-03-C, -03-D and -03-E, not corrected for losses due to backscattering. 2σ-errors include ion statistics, variations in sensitivity, interference corrections and uncertainties in the absolute calibration. The 2σ-error for the average values is given as the 2σ error of the mean and factors for the backscattering corrected average are similar as described above.

Supporting references and notes:

S1. V. Heber, PhD thesis #14579, ETH Zurich (2002), http://e-collection.ethbib.ethz.ch/show?type=diss&nr=14579.

S2. J. F. Ziegler, *Nucl. Instr. Meth. Phys. Res. B* **219-20**, 1027 (2004).

S3. R. C. Wiens, P. Bochsler, D. S. Burnett, R. F. Wimmer-Schweingruber, *Earth Planet. Sci. Lett.* **226**, 549 (2004).

S4. D. B. Reisenfeld *et al.*, paper presented at the 37th Lunar Planet. Sci. Conf., Houston, TX, 14 March 2006.

S5. J. Geiss *et al.*, *Space Sci. Rev.* **110**, 307 (2004).

S6. I. Leya, H.-J. Lange, S. Neumann, R. Wieler, R. Michel, *Meteorit. Planet. Sci.* **35**, 259 (2000).

S7. J.-P. Benkert, H. Baur, P. Signer, R. Wieler, *J. Geophys. Res. (Planets)* **98**, 13147 (1993).